Meteoritics & Planetary Science 51, Nr 2, 429–437 (2016)
doi: 10.1111/maps.12595

Report

Effect of a synchrotron X-ray microtomography imaging experiment on the amino acid content of a CM chondrite

Jon M. FRIEDRICH[1,2,*], Daniel P. GLAVIN[3], Mark L. RIVERS[4], and Jason P. DWORKIN[3]

[1]Department of Chemistry, Fordham University, Bronx, New York 10458, USA
[2]Department of Earth and Planetary Sciences, American Museum of Natural History, New York, New York 10024, USA
[3]Solar System Exploration Division, NASA Goddard Space Flight Center, Greenbelt, Maryland 20771, USA
[4]Center for Advanced Radiation Sources, University of Chicago, Argonne, Illinois 60439, USA
[*]Corresponding author. E-mail: friedrich@fordham.edu

(Received 15 July 2015; revision accepted 09 November 2015)

Abstract–X-ray microcomputed tomography and synchrotron X-ray microcomputed tomography (μCT) are becoming popular tools for the reconnaissance imaging of chondrites. However, there are occasional concerns that the use of μCT may be detrimental to organic components of a chondrite. Soluble organic compounds represent ~2–10% of the total solvent extractable carbon in CI and CM carbonaceous chondrites and amino acids are among the most abundant compounds in the soluble organic fraction. We irradiated two samples of the Murchison CM2 carbonaceous chondrite under conditions slightly harsher (increased beam exposure time) than those typically used for x-ray μCT imaging experiments to determine if detectable changes in the amino acid abundance and distribution relative to a nonexposed control sample occurred. After subjecting two meteorite portions to ionizing radiation dosages of 1.1 kiloGray (kGy) and 1.2 kGy with 48.6 and 46.6 keV monochromatic X-rays, respectively, we analyzed the amino acid content of each sample. Within analytical errors, we found no differences in the amino acid abundances or enantiomeric ratios when comparing the control samples (nonexposed Murchison) and the irradiated samples. We show with calculations that any sample heating due to x-ray exposure is negligible. We conclude that a monochromatic synchrotron X-ray μCT experiment at beamline 13-BM-D of the Advanced Photon Source, which imparts ~1 kGy doses, has no detectable effect on the amino acid content of a carbonaceous chondrite. These results are important for the initial reconnaissance of returned samples from the OSIRIS-REx and Hayabusa 2 asteroid sample return missions.

INTRODUCTION

X-ray microcomputed tomography and synchrotron X-ray microcomputed tomography (μCT) are becoming valuable reconnaissance and research tools in meteoritics and planetary science (Hezel et al. 2013). Reconnaissance investigation of recently fallen (Jenniskens et al. 2012), returned (Tsuchiyama et al. 2011), or inherently rare extraterrestrial samples with μCT has several advantages. Interesting mineralogies, lithologies, or petrographic structures can be identified in 3-D prior to cutting the sample, resulting in critical material conservation and preservation (Ruzicka et al. 2015). Petrography and physical properties can be investigated without the making of traditional petrographic thin sections, whose study can complicate interpretation of complex 3-D structures (Friedrich et al. 2008, 2014).

With respect to chondrites, μCT is generally considered a nondestructive technique. The chemical structures of silicate and metallic minerals are generally unaffected by X-ray exposure at the intensities and wavelengths used for μCT imaging. However, silicate and metallic minerals are not the only constituents of

Table 1. Experimental details of the synchrotron beam exposure and irradiated Murchison CM2 carbonaceous chondrite samples.

Sample	Irradiated mass (g)	Beam exposure duration (min)	Monochromator energy (keV)	Total exposure energy (J)	Dose (Gy)
A	0.5161	64	46.6	0.67	1200
B	0.5091	43	48.6	0.56	1100

chondrites. For example, the subject of this work, the Murchison CM2 carbonaceous chondrite, has a total organic carbon content of ~2.7% (Pearson et al. 2006). The types of organic material in extraterrestrial samples can be divided into soluble and insoluble organic matter. The latter comprises >70% of the total organic carbon and is generally in the form of kerogen-like polycyclic aromatic hydrocarbons (Sephton et al. 2004; Cody and Alexander 2005). The soluble organic material contains a wide range of organic compounds including carboxylic acids, amino acids, sulfonic acids, phosphonic acids, hydroxy acids, aliphatic and aromatic hydrocarbons, polyols, amines, and nitrogen heterocycles (Pizzarello et al. 2006). In Murchison, the total amino acid abundance ranges from ~14 up to 60 $\mu g\ g^{-1}$ (Pizzarello et al. 2006; Glavin et al. 2010).

There is frequent informal debate about the possible effect of high intensity analytical X-ray beams on the abundance and composition of amino acids in chondrites, but little evidence exists. Peripherally related studies have observed that the organic materials of chondrite-like Wild 2 cometary particles may be affected by exposure to high intensity synchrotron microbeam radiation for XANES or XRF data collection (Cody et al. 2009; Wirick et al. 2009). However, microbeam experiments such as these utilize Fresnel zone plate (FZP) or Kirkpatrick-Baez (K-B) mirrors to focus the synchrotron X-ray beam, which yield radiation doses higher than those described in this work. Ebel and Zare (personal communication) observed that polycyclic aromatic hydrocarbon structures were unaffected by synchrotron μCT imaging at the same beamline and under the same conditions as the experiments described in this work. It has been observed that exposure to high energy ionizing radiation such as γ-radiation can destroy amino acids (Kminek and Bada 2006; Iglesias-Groth et al. 2011) and induce racemization of chiral amino acids (Bonner et al. 1979). However, it should be noted that much higher γ-radiation levels (~1 MGy) were used in these experiments compared to the kGy radiation doses commonly imparted during X-ray μCT imaging experiments. In this work, we examine if a routine μCT scan can alter the amino acid content of the Murchison CM chondrite.

MATERIALS AND METHODS

We obtained a single chip of the Murchison CM2 carbonaceous chondrite from the Smithsonian National Museum of Natural History, Washington DC (USNM 5453, total mass 15.2 g). The entire chip was crushed to a powder (estimated <150 μm) and manually homogenized with a mortar and pestle in a positive pressure high efficiency particulate air (HEPA) filtered laminar flow hood. All glassware, ceramics, and sample handling tools were wrapped in aluminum foil and then pyrolyzed in a furnace in air at 500 °C overnight. Two ~0.5 g aliquots of the Murchison powder "A" and "B" (Table 1) were transferred to separate borosilicate glass vials (~1 cm outer diameter) and sealed with a pyrolyzed aluminum foil lined cap under air for the X-ray imaging experiment. All sample processing was performed under clean conditions at the Goddard Space Flight Center (GSFC) and the vials remained sealed from the time they left GSFC to the time they returned to GSFC for amino acid extraction and analysis.

For irradiation, we used the X-ray microtomography apparatus at the 13-BM-D bending magnet beamline of the GeoSoilEnviroCARS (GSECARS) facility at the Advanced Photon Source (APS), a third generation synchrotron light source at Argonne National Laboratory. Parameters for the X-ray microtomography experiment are akin to those commonly used for the imaging of chondritic meteorites at this beamline (see Ebel and Rivers 2007; Friedrich et al. 2008, 2014). We used monochromatic X-rays at 46.6 and 48.6 keV for Murchison samples A and B, respectively (Table 1). These two energies were selected because they are typical for those needed for penetrating samples of the size and composition of those used for these experiments. To intensify any possible effect on the amino acid content, we used slightly longer beam exposure times than typically used at beamline 13-BM-D for synchrotron μCT imaging experiments (Table 1). Each sample was imaged and then left in the beam for an additional period of time.

Following the X-ray imaging experiments, a portion of each exposed sample (sample A, mass 107.7 mg; sample B, mass 130.9 mg) along with a nonexposed Murchison control sample (mass 126.8 mg) were flame-sealed

separately in glass ampoules in 1 mL of Millipore Direct Q3 UV (18.2 MΩ, <5 ppb total organic carbon) ultrapure water and extracted at 100 °C for 24 h. A crushed serpentine sample (516.0 mg) that had been heated in air at 500 °C overnight was taken through the same extraction procedure as the meteorite samples and used as a procedural blank. Half of the water supernatants were then subjected to a 6M HCl acid vapor hydrolysis procedure at 150 °C for 3 h to determine the total hydrolyzable amino acid content (Glavin et al. 2006), while the other half was not hydrolyzed to determine the free amino acid content. Both acid-hydrolyzed and nonhydrolyzed water extracts were then desalted using prepacked cation-exchange columns (AG50W-X8, 100-200 mesh, hydrogen form, BIO-RAD) and the amino acid fraction recovered by elution with NH_4OH and concentrated by drying under vacuum. The desalted extracts were derivatized with *o*-phthaldialdehyde/N-acetyl-L-cysteine (OPA/NAC) and the OPA/NAC amino acid derivatives analyzed by ultrahigh-performance liquid chromatography with UV fluorescence detection and time of flight mass spectrometry (LC-FD/ToF-MS). Additional details of the amino acid work-up and LC-FD/ToF-MS experimental conditions are described elsewhere (Glavin et al. 2010). Amino acid abundances and their enantiomeric ratios in the meteorite extracts were determined by comparison of the peak areas generated from the UV fluorescence detector and ToF-MS of the OPA/NAC amino acid derivatives to the corresponding areas of standards run under the same chromatographic conditions on the same day. The free and total amino acid concentrations in the sample extracts were then determined from the average of between three to six separate UPLC-FD/ToF-MS measurements.

RESULTS AND DISCUSSION

Dosage Calculation

If amino acids were the only component of the material, we could, in principle, calculate an absorbed dose for the amino acids themselves. However, the amino acids in a carbonaceous chondrite are not present as isolated materials. The exact provenance of the amino acids and other soluble organics in meteorites is not well known. The fact that most of the soluble organic matter in carbonaceous chondrites becomes extractable only after demineralization suggests that a significant fraction of the soluble organics are trapped in interlayer sites or on grain boundaries between minerals (Becker and Epstein 1982). It is not just the X-rays absorbed by the amino acid that are important for their potential degradation, but the total X-rays absorbed by the system. Impinging X-rays will interact with the amino acids themselves, but also deposit energies into minerals by a variety of mechanisms including inelastic scattering, photoelectron emission and absorption, Auger electrons, and X-ray fluorescence. These secondary particles will have a mean free path much larger than the ionization cross section of an amino acid (Scheer et al. 2007). So, X-rays stopped by a host or neighboring mineral will generate electrons that may damage the amino acid. This will especially be the case for secondary electrons near the C, N, and O X-ray K-edges at energies of 285–600 eV.

The total radiation dose experienced by Murchison sample A is calculated using the experimental parameters shown in Table 1. In the case of the 46.6 keV used for Murchison sample A, to calculate the total radiation dose begin with the number of X-ray photons hitting the sample per second. At that energy, the intensity of the X-ray beam from the source is equivalent to 4×10^{13} photons s^{-1} $mrad^{-2}$/0.1% bandwidth. The sample and X-ray imaging apparatus is located 56 m away from the synchrotron source and the sample had a horizontal field of view of 10 mm and a vertical field of view of 2.5 mm. This yields an angular field of view for the sample of 8×10^{-3} $mrad^2$. The monochromator bandwidth is approximately 0.01%. Taken together, these factors yield 3.2×10^{10} photons s^{-1} interacting with the sample. By taking the difference between the count rate with no sample in the beam path and the central portion of the beam with the sample present in the beam path, we measured ~30%, on average, of the X-ray flux being transmitted through the sample, leaving 2.2×10^{10} photons being absorbed by the sample. In terms of energy, this is equivalent to 1.6×10^{-4} J s^{-1}. Given the sample size and exposure duration (Table 1), we find a dose of 1200 Gray for Murchison sample A. A similar calculation yields a dose of 1100 Gy for Murchison sample B (Table 1). In that case, the 48.6 keV energy, intensity, and exposure time are different. The other parameters are the same.

We note that these doses are likely similar to those imparted at other third generation synchrotron facilities performing projection tomography experiments like those used here (e.g., Uesugi et al. 2013). However, sophisticated high spatial resolution X-ray microtomography experiments using FZP lenses (e.g., Tsuchiyama et al. 2011) will impart significantly higher dosages to a sample—up to an order of magnitude higher (K. Uesugi and Tsuchiyama, personal communication). Caution should be used for extrapolating our results to experimental apparatuses employing focusing X-ray lenses because the dose will unquestionably be higher.

Sample Heating during Irradiation

Because we used powdered samples that were kept sealed in glass vials to minimize contamination, we were unable to attach a thermocouple to the sample to evaluate the possible role of sample heating in altering the chemical make-up of the sample. However, because we have calculated the energy imparted into the sample, we can use that to estimate a temperature rise of the sample. A typical specific heat capacity for carbonaceous chondrites has been measured to be on the order of 0.5 J g^{-1} °C (Matsui and Osako 1979; Opeil et al. 2010, 2012; Szurgot 2011). Given the 0.67 J imparted and mass of the sample (Table 1), this yields a temperature increase of 2.6 °C for Murchison sample A. A similar calculation finds Murchison sample B to have 2.2 °C rise in temperature. However, these values assume all of the energy stays in the sample during the entire duration of the experiment—the thermal conductivity of the sample is zero and there is no transfer of energy by conduction to the air and sample holder. These estimates further assume that the X-rays are absorbed evenly by the entire sample and there are no regions with higher absorption or localized heating. Finally, we point out that the specific heat capacity of amino acids is ~1.3 J g^{-1} °C (Domalski and Hearing 1996), higher than the carbonaceous chondrite as a whole. Taken together, we estimate that the actual maximum temperature experienced by the sample as a whole was <1 °C above the controlled temperature on the APS experiment floor or <23 °C. Regardless, the thermal degradation of amino acids in dry Murchison samples is minimal below 160 °C (Rodante et al. 1992).

Amino Acid Content

We quantified the abundances of 13 amino acids, including the enantiomers of 7 amino acids from the LC-FD and ToF-MS data. Typical LC-FD chromatograms of the 6M HCl acid hydrolyzed, hot-water extracts from the X-ray exposed Murchison A sample, the nonirradiated Murchison control sample, the serpentine blank, and an amino acid standard mixture are shown in Fig. 1. The identified amino acids and corresponding abundances are given in Table 2. Only trace levels of background amino acids were identified in the LC-FD chromatograms of the serpentine blank sample. The abundances of amino acids reported in Table 2 for the two irradiated samples and the control sample were background corrected using the serpentine blank. Abundances of total individual amino acids or their enantiomers relative to the control sample are shown in Fig. 2. Since the irradiation conditions (Table 1) and the results are similar for the two replicate samples (Table 2) we show the average of the results in Fig. 2 (also see Table 2 for the means). The uncertainties reported are based on the standard errors of the average value of between three to six separate measurements of the meteorite extracts. It should be noted that the total amino acid abundances and enantiomeric ratios of the Murchison control sample analyzed in this study were essentially identical to a prior analysis of the hot-water extract from a different aliquot of the same powdered sample (Glavin et al. 2010), indicating that the powdered Murchison sample is homogeneous with respect to the amino acid content (at least at the ~100–130 mg sample size scale). The amino acid abundances are identical within error in the irradiated and control samples except for L-glutamic acid (L-Glu), L-β-amino-*n*-butyric acid (L-β-ABA), and L-serine (L-Ser) (Fig. 2). In the case of L-Glu and L-β-ABA, the results overlap at the 2σ error level. Irradiated samples are slightly enriched in L-Glu and L-β-ABA relative to the control sample (Fig. 2). L-Ser shows a more substantial increase in our irradiated sample relative to the control sample. We attribute this excess to contamination since L-Ser is a commonly occurring terrestrial amino acid contaminant. We note that the D/L-Ser ratios for the free amino acids for the averages of the amino acid analyses of irradiated samples A and B are nearly identical.

We analyzed the abundances of 13 different amino acids, including the enantiomeric ratios of seven chiral amino acids in our two irradiated samples and control sample and the results are shown in Tables 2 and 3. The normalized enantiomeric ratios for each sample (relative to the Murchison control) are shown in Fig. 3. Within analytical error, the D/L ratios of the amino acids in the irradiated and control samples show in Fig. 3 are identical. The most aberrant case (D/L-Ser) can be attributed to an elevated L-Ser abundance in one of our irradiated sample replicates (Murchison B—see Table 2). Therefore, based on our experimental data, we conclude that irradiation of the Murchison meteorite using the experimental apparatus and parameters used in our imaging experiments does not alter the free or total amino acid abundances or enantiomeric ratios originally present in the powdered meteorite sample.

CONCLUSIONS

We have irradiated two samples of the Murchison CM2 chondrite with monochromatic synchrotron X-rays at beamline 13-BM-D at the APS at energies typical for μCT imaging of extraterrestrial samples. The total dose of radiation was 1.1 kiloGray (kGy) and 1.2 kGy with energies of 48.6 and 46.6 keV,

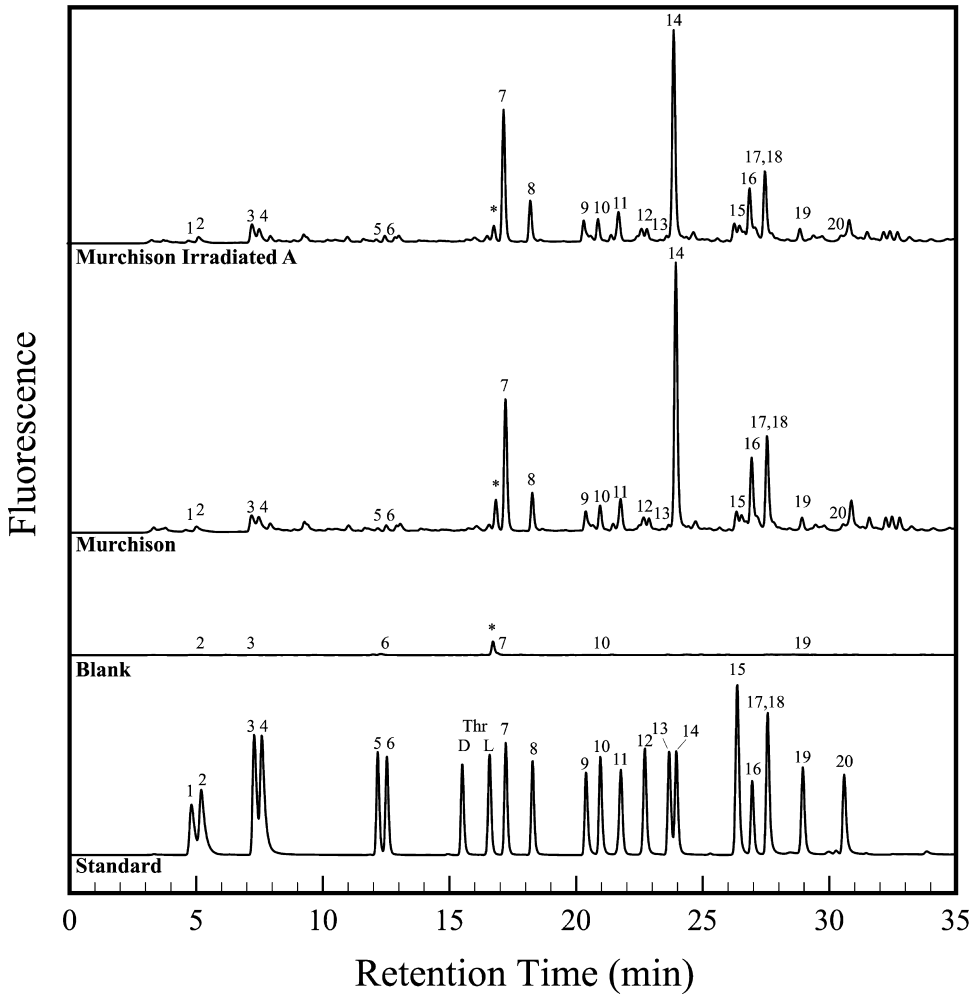

Fig. 1. The 0- to 35-min region of the LC-FD chromatograms. OPA/NAC derivatization (15 min) of a standard and the 6 M HCl-hydrolyzed, hot-water extracts of the irradiated Murchison sample A, the unirradiated Murchison, and an unirradiated pyrolyzed serpentine blank carried through the same workup as the Murchison samples. Each derivatized sample was analyzed using our standard tandem LC column setup including a Waters BEH C18 column (2.1 × 50 mm, 1.7 μm bead) followed by a second Waters BEH Phenyl-Hexyl column (2.1 × 150 mm, 1.7 μm bead). The conditions for separation of the OPA/NAC amino acid derivatives at 30 °C were as follows: flow rate, 150 μl min^{-1}; solvent A (50 mM ammonium formate, 8% methanol, pH 8.0); solvent B (methanol); gradient, time in minutes (%B): 0 (0), 35 (55), 45 (100). Peaks in the chromatograms that did not correspond to the same UV fluorescence and mass retention times of the standard amino acids tested were not identified. Peak identifications: 1, D-aspartic acid; 2, L-aspartic acid; 3, L-glutamic acid; 4, D-glutamic acid; 5, D-serine; 6, L-serine; 7, glycine; 8, β-alanine; 9, γ-amino-*n*-butyric acid; 10, D-alanine; 11, L-alanine; 12, D-β-amino-*n*-butyric acid; 13, L-β-amino-*n*-butyric acid; 14, α-aminoisobutyric acid; 15, D,L-α-amino-n-butyric acid; 16, D-isovaline; 17 + 18, L-isovaline + ε-amino-*n*-caproic acid (separated by mass for quantification); 19, L-valine; 20, D-valine. The standard also contains D and L-threonine (Thr), a common protein amino acid. The peak marked with * indicates a fluorescent artifact from the workup.

respectively. Under these conditions, we found that the abundances and enantiomeric ratios of the targeted amino acids extracted from irradiated Murchison samples were within analytical errors of the measurements made on the control Murchison sample. We conclude that a synchrotron X-ray microtomography experiment at beamline 13-BM-D at the APS under the conditions listed in Table 1 has no discernable effect on the free and total amino acid content of a powdered carbonaceous chondrite. These data provide confidence in the use of μCT experiments similar to those undertaken at beamline 13-BM-D at the APS for the preliminary analysis of returned samples from the OSIRIS-REx and Hayabusa 2 missions.

Acknowledgments—The authors thank T. McCoy and L. Welzenbach who kindly allocated the Murchison meteorite sample used in this study. JMF would like to

Table 2. Summary of the average procedural blank-corrected free (nonhydrolyzed) and total (6M HCl acid hydrolyzed) amino acid concentrations in the hot-water extracts of powdered aliquots of a nonirradiated control sample compared to an X-ray irradiated Murchison sample (USNM 5453)[a].

	Murchison (control)		Murchison irradiated sample A		Murchison irradiated sample B		Murchison irradiated mean	
Amino Acid	Free (ng g^{-1})	Total (ng g^{-1})	Free (ng g^{-1})	Total (ng g^{-1})	Free (ng g^{-1})	Total (ng g^{-1})	Free (ng g^{-1})	Total (ng g^{-1})
D-Aspartic acid	26 ± 4	140 ± 21	31 ± 11	180 ± 37	30 ± 5	165 ± 10	31 ± 7	174 ± 24
L-Aspartic acid	46 ± 4	339 ± 32	70 ± 17	337 ± 47	70 ± 9	391 ± 34	70 ± 11	360 ± 33
D-Glutamic acid	31 ± 4	532 ± 46	45 ± 7	521 ± 66	36 ± 12	553 ± 26	42 ± 6	533 ± 44
L-Glutamic acid	60 ± 12	741 ± 84	80 ± 23	812 ± 96	97 ± 33	1090 ± 163	86 ± 19	917 ± 100
D-Serine	20 ± 3	62 ± 9	28 ± 7	58 ± 17	21 ± 1	50 ± 13	25 ± 5	55 ± 12
L-Serine	89 ± 41	151 ± 25	40 ± 13	180 ± 28	329 ± 49	364 ± 63	149 ± 60	249 ± 46
Glycine	1009 ± 141	2275 ± 300	1266 ± 300	2883 ± 620	820 ± 30	2416 ± 305	1117 ± 220	2750 ± 477
D-Alanine	400 ± 64	848 ± 102	425 ± 76	910 ± 133	267 ± 26	919 ± 70	372 ± 60	913 ± 88
L-Alanine	399 ± 84	982 ± 126	457 ± 109	1100 ± 193	281 ± 61	1082 ± 117	399 ± 84	1094 ± 130
β-Alanine	535 ± 80	1,459 ± 195	566 ± 102	1528 ± 298	361 ± 46	1644 ± 160	498 ± 80	1578 ± 205
D+L-α-Amino-*n*-butyric acid[b]	231 ± 48	756 ± 62	293 ± 39	706 ± 118	193 ± 20	732 ± 161	259 ± 33	716 ± 94
D-β-Amino-*n*-butyric acid	113 ± 15	258 ± 33	133 ± 24	282 ± 39	72 ± 7	271 ± 27	109 ± 19	277 ± 25
L-β-Amino-*n*-butyric acid	95 ± 12	207 ± 17	87 ± 13	230 ± 19	90 ± 11	262 ± 16	88 ± 9	244 ± 15
γ-Amino-*n*-butyric acid	252 ± 54	901 ± 129	289 ± 103	1,109 ± 158	129 ± 21	778 ± 178	235 ± 76	985 ± 136
α-Aminoisobutyric acid	5067 ± 944	5822 ± 267	5658 ± 1506	5315 ± 1047	3631 ± 151	5781 ± 373	4983 ± 978	5515 ± 649
D-Isovaline	3142 ± 494	3606 ± 313	3509 ± 767	3946 ± 696	1943 ± 98	3826 ± 261	2987 ± 595	3901 ± 455
L-Isovaline	3652 ± 562	4078 ± 403	4227 ± 824	4598 ± 915	1863 ± 30	4480 ± 295	3439 ± 702	4554 ± 593
D-Valine	99 ± 18	248 ± 52	86 ± 15	231 ± 16	164 ± 51	260 ± 25	112 ± 23	243 ± 16
L-Valine	167 ± 34	486 ± 56	124 ± 22	465 ± 58	337 ± 113	468 ± 69	195 ± 53	466 ± 47
ε-Amino-*n*-caproic acid	90 ± 15	489 ± 124	100 ± 36	515 ± 153	105 ± 23	312 ± 70	102 ± 23	413 ± 96

[a]The uncertainties are based on the standard errors of the average value of 3–6 separate measurements of the hot-water extracts of the same powdered meteorite sample.
[b]Enantiomers could not be separated under the chromatographic conditions used for this study.

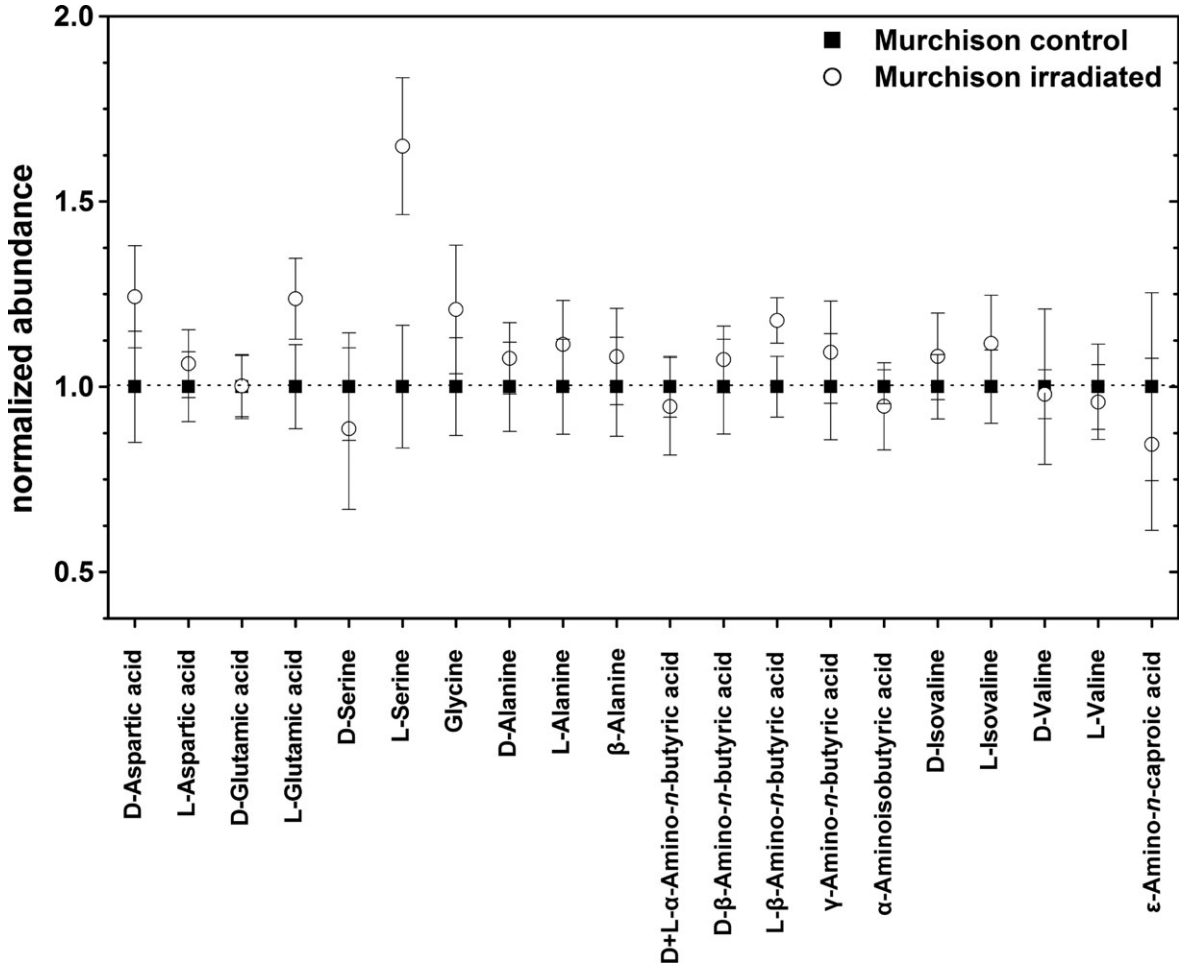

Fig. 2. Total amino acid abundances in the irradiated Murchison samples (average of A and B) normalized to the control Murchison sample. The uncertainties are based on the standard deviation of the average value of between three and six separate measurements (N) with a standard error $\delta x = \sigma_x \cdot (N - 1)^{-1/2}$.

Table 3. Amino acid enantiomeric ratios (D/L) measured in the free (nonhydrolyzed) and total (6M HCl acid hydrolyzed) hot-water extracts of the control and X-ray exposed Murchison meteorite USNM 5453[a].

	Murchison (control)		Murchison irradiated sample A		Murchison irradiated sample B		Murchison irradiated mean	
Sample	Free	Total	Free	Total	Free	Total	Free	Total
D/L-Aspartic acid	0.57 ± 0.11	0.41 ± 0.07	0.44 ± 0.19	0.53 ± 0.13	0.44 ± 0.09	0.42 ± 0.04	0.44 ± 0.12	0.48 ± 0.08
D/L-Glutamic acid	0.52 ± 0.12	0.72 ± 0.10	0.57 ± 0.18	0.64 ± 0.11	0.37 ± 0.17	0.51 ± 0.08	0.48 ± 0.12	0.58 ± 0.08
D/L-Serine	0.22 ± 0.11	0.41 ± 0.09	0.68 ± 0.28	0.32 ± 0.11	0.06 ± 0.01	0.14 ± 0.04	0.17 ± 0.07	0.22 ± 0.06
D/L-Alanine	1.00 ± 0.26	0.86 ± 0.15	0.93 ± 0.28	0.83 ± 0.19	0.80 ± 0.13	0.85 ± 0.11	0.93 ± 0.24	0.84 ± 0.13
D/L-β-Amino-*n*-butyric acid	1.19 ± 0.22	1.25 ± 0.19	1.53 ± 0.36	1.23 ± 0.20	0.80 ± 0.12	1.03 ± 0.12	1.17 ± 0.24	1.13 ± 0.16
D/L-Isovaline	0.86 ± 0.19	0.88 ± 0.12	0.83 ± 0.24	0.86 ± 0.22	1.04 ± 0.06	0.85 ± 0.08	0.87 ± 0.24	0.86 ± 0.15
D/L-Valine	0.59 ± 0.16	0.51 ± 0.12	0.69 ± 0.17	0.50 ± 0.07	0.49 ± 0.22	0.55 ± 0.10	0.57 ± 0.19	0.52 ± 0.06

[a]Uncertainties in the D/L ratios were calculated by standard error propagation of the absolute errors shown in Table 1.

thank the Camille and Henry Dreyfus Special Grant Program in the Chemical Sciences for providing vital material support. Portions of this work were performed at GeoSoilEnviroCARS (Sector 13), Advanced Photon Source (APS), Argonne National Laboratory. GeoSoilEnviroCARS is supported by the National

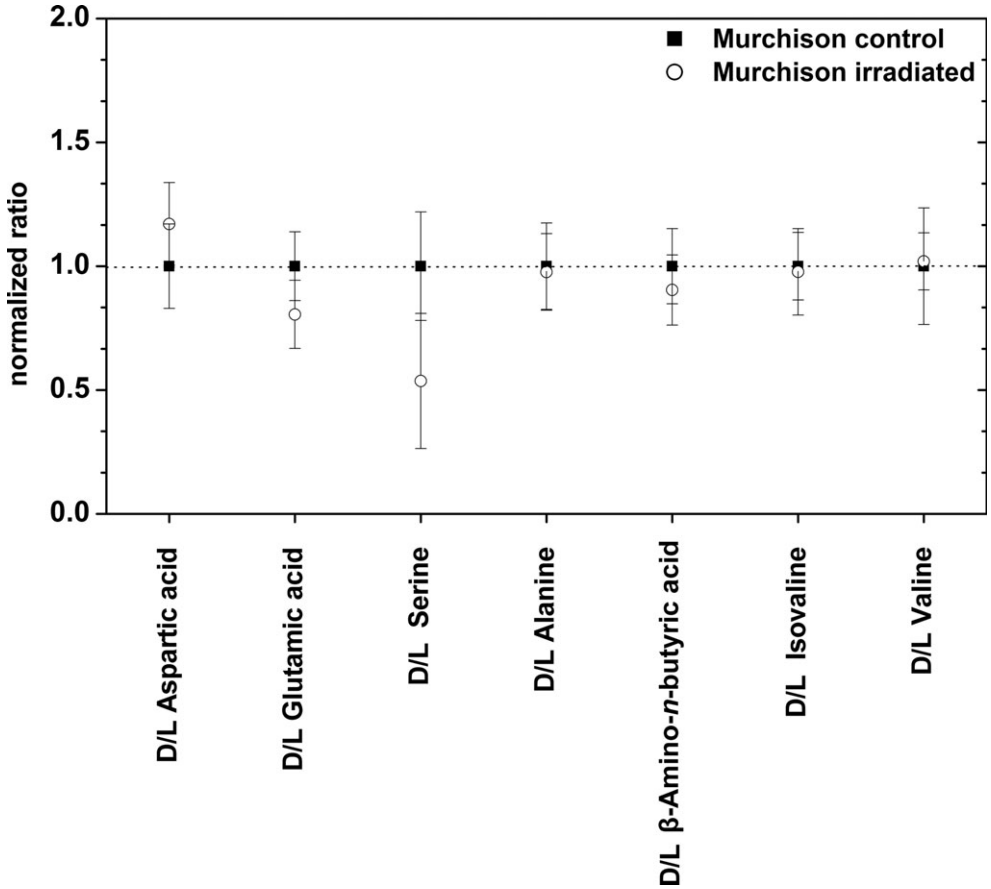

Fig. 3. Enantiomeric ratios of total amino acids in hot-water, acid-hydrolyzed extracts of the irradiated Murchison samples (average of A and B) relative to the control Murchison sample. Errors shown are based on the standard deviation of the average value of between three and six separate measurements.

Science Foundation—Earth Sciences (EAR-1128799) and Department of Energy-GeoSciences (DE-FG02-94ER14466). This research used resources of the Advanced Photon Source, a U.S. Department of Energy (DOE) Office of Science User Facility operated for the DOE Office of Science by Argonne National Laboratory under Contract No. DE-AC02-06CH11357. DPG and JPD appreciate funding support from the NASA Astrobiology Institute and the Goddard Center for Astrobiology and Hannah McLain for technical support.

The authors thank Dr. A. Tsuchiyama for a thorough review and Dr. S. Sandford for swift editorial handling.

Editorial Handling—Dr. Scott Sandford

REFERENCES

Becker R. H. and Epstein S. 1982. Carbon, hydrogen and nitrogen isotopes in solvent-extractable organic matter from carbonaceous chondrites. *Geochimica et Cosmochimica Acta* 46:97–103.

Bonner W. A., Blair N. E., and Lemmon R. M. 1979. The radioracemization of amino acids by ionizing radiation: Geochemical and cosmochemical implications. *Origins of Life* 9:279–290.

Cody G. D. and Alexander C. M. O'D. 2005. NMR studies of chemical structural variation of insoluble organic matter from different carbonaceous chondrite groups. *Geochimica et Cosmochimica Acta* 69:1085–1097.

Cody G. D., Brandes J., Jacobson C., and Wirick S. 2009. Soft X-ray induced chemical modification of polysaccharides in vascular plant cell walls. *Journal of Electron Spectroscopy and Related Phenomena* 170:57–64.

Domalski E. S. and Hearing E. D. 1996. Heat capacities of organic compounds in the condensed phase. Volume III. *Journal of Physical Chemistry Reference Data* 25: 1–523.

Ebel D. S. and Rivers M. L. 2007. Meteorite 3-dimensional synchrotron microtomography: Methods and applications. *Meteoritics & Planetary Science* 42:1627–1646.

Friedrich J. M., Wignarajah D. P., Chaudhary S., Rivers M. L., Nehru C. E., and Ebel D. S. 2008. Three-dimensional petrography of metal phases in equilibrated L chondrites–Effects of shock loading and dynamic compaction. *Earth and Planetary Science Letters* 275:172–180.

Friedrich J. M., Weisberg M. K., and Rivers M. L. 2014. Multiple impact events recorded in the NWA 7298 H

chondrite breccia and the dynamical evolution of an ordinary chondrite asteroid. *Earth and Planetary Science Letters* 394:13–19.

Glavin D. P., Dworkin J. P., Aubrey A., Botta O., Doty J. H. III, Martins Z., and Bada J. L. 2006. Amino acid analyses of Antarctic CM2 meteorites using liquid chromatography-time of flight-mass spectrometry. *Meteoritics & Planetary Science* 41:889–902.

Glavin D. P., Callahan M. P., Dworkin J. P., and Elsila J. E. 2010. The effects of parent body processes on amino acids in carbonaceous chondrites. *Meteoritics & Planetary Science* 45:1948–1972.

Hezel D. C., Friedrich J. M., and Uesugi M. 2013. Looking inside: 3D structures of meteorites. *Geochimica et Cosmochimica Acta* 116:1–4.

Iglesias-Groth S., Cataldo F., Ursini O., and Manchado A. 2011. Amino acids in comets and meteorites: Stability under gamma radiation and preservation of the enantiomeric excess. *Monthly Notices of the Royal Astronomical Society* 410:1447–1453.

Jenniskens P., Fries M. D., Yin Q.-Z., Zolensky M., Krot A. N., Sandford S. A., Sears D., Beauford R., Ebel D. S., Friedrich J. M., Nagashima K., Wimpenny J., Yamakawa A., Nishiizumi K., Hamajima Y., Caffee M. W., Welten K. C., Laubenstein M., Davis A. M., Simon S. B., Heck P. R., Young E. D., Kohl I. E., Thiemens M. H., Nunn M. H., Mikouchi T., Hagiya K., Ohsumi K., Cahill T. A., Lawton J. A., Barnes D., Steele A., Rochette P., Verosub K. L., Gattacceca J., Cooper G., Glavin D. P., Burton A. S., Dworkin J. P., Elsila J. E., Pizzarello S., Ogliore R., Schmitt-Kopplin P., Harir M., Hertkorn N., Verchovsky A., Grady M., Nagao K., Okazaki R., Takechi H., Hiroi T., Smith K., Silber E. A., Brown P. G., Albers J., Klotz D., Hankey M., Matson R., Fries J. A., Walker R. J., Puchtel I., Lee C.-T. A., Erdman M. E., Eppich G. R., Roeske S., Gabelica Z., Lerche M., Nuevo M., Girten B., and Worden S. P. 2012. Radar-enabled recovery of the Sutter's Mill meteorite, a carbonaceous chondrite regolith breccia. *Science* 338:1583–1587.

Kminek G. and Bada J. L. 2006. The effect of ionizing radiation on the preservation of amino acids on Mars. *Earth and Planetary Science Letters* 245:1–5.

Matsui T. and Osako M. 1979. Thermal property measurement of Yamato meteorites. *Memoirs of National Institute of Polar Research Special Issue* 15:243–252.

Opeil C. P., Consolmagno G. J., and Britt D. T. 2010. The thermal conductivity of meteorites: New measurements and analysis. *Icarus* 208:449–454.

Opeil C. P., Consolmagno G. J., Safarik D. J., and Britt D. T. 2012. Stony meteorite thermal properties and their relationship to meteorite chemical and physical states. *Meteoritics & Planetary Science* 47:319–329.

Pearson V. K., Sephton M. A., Franchi I. A., Gibson J. M., and Gilmour I. 2006. Carbon and nitrogen in carbonaceous chondrites: Elemental abundances and stable isotopic compositions. *Meteoritics & Planetary Science* 41:1899–1918.

Pizzarello S., Cronin J. R., and Flynn G. 2006. The nature and distribution of organic material in carbonaceous chondrites and interplanetary dust particles. In *Meteorites and the early solar system II*, edited by Lauretta D. S. Tucson, Arizona: The University of Arizona Press. pp. 625–652.

Rodante F., Marrosu G., and Catalani G. 1992. Thermal analysis of some α-amino acids with similar structures. *Thermochimica Acta* 194:197–213.

Ruzicka A., Brown R., Friedrich J., Hutson M., Hugo R., and Rivers M. (2015). Shock-induced mobilization of metal and sulfide in planetesimals: Evidence from the Buck Mountains 005 (L6 S4) dike-bearing chondrite. *American Mineralogist* 100:2725–2738.

Scheer A. M., Mozejko P., Gallup G. A., and Burrow P. D. 2007. Total dissociative electron attachment cross sections of selected amino acids. *The Journal of Chemical Physics* 126:174301.

Sephton M. A., Bland P. A., Pillinger C. T., and Gilmour I. 2004. The preservation state of organic matter in meteorites from Antarctica. *Meteoritics & Planetary Science* 39:747–754.

Szurgot M. 2011. On the specific heat capacity and thermal capacity of meteorites (abstract #1150). 42nd Lunar and Planetary Science Conference. CD-ROM.

Tsuchiyama A., Uesugi M., Matsushima T., Michikami T., Kadono T., Nakamura T., Uesugi K., Nakano T., Sandford S. A., Noguchi R., Matsumoto T., Matsuno J., Nagano T., Imai Y., Takeuchi A., Suzuki Y., Ogami T., Katagiri J., Ebihara M., Ireland T. R., Kitajima F., Nagao K., Naraoka H., Noguchi T., Okazaki R., Yurimoto H., Zolensky M. E., Mukai T., Abe M., Yada T., Fujimura A., Yoshikawa M., and Kawaguchi J. 2011. Three-dimensional structure of Hayabusa samples: Origin and evolution of Itokawa regolith. *Science* 333:1125–1128.

Uesugi M., Uesugi K., Takeuchi A., Suzuki Y., Hoshino M., and Tsuchiyama A. 2013. Three-dimensional observation of carbonaceous chondrites by synchrotron radiation X-ray CT—Quantitative analysis and developments for the future sample return missions. *Geochimica et Cosmochimica Acta* 116:17–32.

Wirick S., Flynn G. J., Keller L. P., Nakamura-Messenger K., Peltzer C., Jacobson C., Sandford S., and Zolensky M. 2009. Organic matter from comet 81P/Wild 2, IDPs, and carbonaceous meteorites; similarities and differences. *Meteoritics & Planetary Science* 44:1611–1626.